

ANALYSIS OF THERMAL TRANSPORT THROUGH A FLAT-PLATE SOLAR COLLECTOR INTEGRATED WITH METAL-FOAM BLOCKS

Ahmed ALBOJAMAL

University of California-Riverside

aalbojamal@engr.ucr.edu

Arman HAGHIGHI*

University of California-Riverside

ahaghghi@engr.ucr.edu

Hudhaifa HAMZAH

University of Mosul

hudhaifahamzah@gmail.com

ABSTRACT: Forced convective heat transfer in a solar water collector channel with three metal-foam blocks attached on the inside wall, is studied numerically. Darcy equation with the Brinkman and Forchheimer terms is used to analyze the flow in the porous section; and Local thermal equilibrium (LTE) is considered between the working fluid and the porous region. The fluid flow in the channel and the thermal behavior of the system are analyzed considering various parameters such as Darcy number, thermal conductivity ratio, porosity and Reynolds number. The results prevail that the generated recirculation zones between blocks will significantly improve the heat transfer rate from the heated surface; and metallic porous material can perform as effective heat exchangers in thermal applications such as electronic cooling and solar heat collectors.

Keywords: solar collector, metal foam, electronic cooling.

Nomenclature

A	aspect ratio, $A = H / H_m$	T	temperature [K]
C	inertia coefficient	U	dimensionless axial velocity
c_p	specific heat [$J / kg \cdot K$]	u	axial velocity [m/s]
Da	Darcy number	V	dimensionless transverse velocity
D_h	hydraulic diameter [m]	v	transverse velocity [m/s]
d_f	fiber diameter [m]	w	width [m]
d_p	mean pore diameter [m]	X	dimensionless axial coordinate
F	Forchheimer coefficient	x	axial coordinate [m]
G	shape function	Y	dimensionless transverse coordinate
H	channel height [m]	y	transverse coordinate [m]
h	local heat transfer coefficient [$W / m^2 K$]		
K	permeability of the porous blocks [m^2]		

Greek symbols

k	fluid thermal conductivity [W / mK]	ε	porosity
L	total length [m]	μ	dynamic viscosity [$Pa \cdot s$]
L_h	length of absorber plate under solar energy [m]	θ	dimensionless
Nu	Nusselt number	ε	temperature
P	dimensionless pressure	ρ	porosity
p	pressure [N / m^2]		density [kg / m^3]
Pr	Prandtl number		
q''	solar heat flux [W / m^2]	e	outlet conditions
R_c	thermal conductivity ratio	eff	effective
Re	Reynolds number	f	fluid
R_x	length ratio, $R_x = W_m / (W_m + S_m)$	m	metal foam
R_y	height ratio, $R_y = H_m / H$	o	inlet conditions
S	spacing [m]	s	solid

Subscripts

* Corresponding author (Address all correspondence to:
aahaghghi@email.ucr.edu)

INTRODUCTION

Thermal efficiency enhancement of heat exchanger has received significant attention by the researchers in order to meet the increasing demand to design and implement compact heat exchangers. Different techniques are utilized by the researchers presented in (Albojamal and Vafai, 2017; Wang and Chen, 2002; Chabane, 2014 and Lee and Vafai, 1999) for heat transfer enhancement. Some of them increase the overall thermal conductivity of the working fluid by dispersing small colloidal solid particles, 1-100 nm in diameter. While others worked on altering the surface geometry by using special channel wall shapes such as wavy or corrugated walls.

Direct solar radiation is one of the promising sources of renewable energy. Solar thermal collectors are a special type of heat exchangers that absorb the incoming solar radiation energy, and transfer it to the internal transport medium (Kalogirou, 2004). Flat-plate collectors are the most common type used in residential structures, space heating, and commercial or industrial applications where the demand for hot water has a large impact on energy costs (Kudish, 2002). There is a lot of effort focused on optimizing the flat-plate solar collector by means of reducing their size and increasing the fluid temperature at the outlet. With this goal, various different techniques have been introduced (Bashria et al., 2007; Chabane, 2014; Reddy and Satyanarayana, 2008). Despite the attractive thermal performance of these techniques, heat transfer in flat plate solar collectors still needs further development to reach higher heat transfer rates between heated surface and the fluid.

Metallic porous material has emerged over the past decade as a promising new technology for a wide range of applications, such as in compact heat sinks in electronic devices, chemical reformers, combustors and solar thermal collectors. This is due to the attractive thermo-mechanical features of metal-foams including high solid thermal conductivity, lightweight with high strength and rigidity, enhanced flow mixing capabilities of porous matrix and large surface area per unit volume (Lu et al., 1998; Banhart, 2001 and Zhao, 2012). Numerous studies have been carried out on forced convection with steady state flow through a channel partially or fully filled with a metal foam (Qu et al., 2012 and Lu et al., 2017). Angirasa (2002) presented a numerical study for heat transfer in a channel completely filled with rigid metallic materials with high porosity. Lu et al. (2006) analytically investigated the open-cell metal foam fully filled heat exchanger pipes. Their results confirmed that the use of metal-foam can dramatically enhance the heat transfer, but at the expense of a significant increase in the pressure drop. They showed that the pressure loss is three to four times higher than that of an empty channel. This situation impairs the application of metal foams for most engineering cases requiring low pressure drop. Also, for fully filled channel LTNE model is more accurate and should be used for the flow analysis according to Lee and Vafai (1999). While for partially filled duct, due to the relatively low velocity in the foam region, the temperature difference between solid and fluid phases is minimal and the LTE model may be employed (Xu et al., 2015).

Present study aims to numerically investigate the characteristics of fluid flow and heat transfer through a parallel flat-plate channel solar water collector with multiple metal-foam blocks mounted on the inside wall and by considering Local Thermal Equilibrium (LTE) in the solid-fluid interface. The essential heat and flow interaction between the metal-foam porous block and the working fluid, as well as the methodology of improving the rate of heat transfer near the heated surface and reduced the pressure drop are analyzed and discussed in this work. Our results were compared and validated with the numerical work of (Chikh et al. 1998).

MATHEMATICAL FORMULATION

The schematic for flat-plate solar collector for forced convection water flow is shown in figure 1 for current study. The water flow through a horizontal parallel-plate channel with three separate metal-foam porous blocks with height H_m and width W_m . The channel height is H and the total length is L . Constant heat flux q'' is imposed along the length of the absorber plate of length L_h . The remaining walls are insulated. The height (R_y) and length (R_x) ratios of the channel are set equal to 0.5 and 0.25 respectively. While the block width (W_m) and the spacing between them (S_m) set equal to each other. Furthermore, the fluid enters the channel with uniform inlet temperature T_o and parabolic fully developed velocity profile. A two-dimensional, laminar, incompressible and steady flow with constant thermophysical properties for both the fluid and metal-foam are considered. The buoyancy and radiation effects are neglected. Also, the porous

metals are considered as homogenous and isotropic. The area after the last block is chosen to be long enough to ensure fully developed conditions at the channel exit.

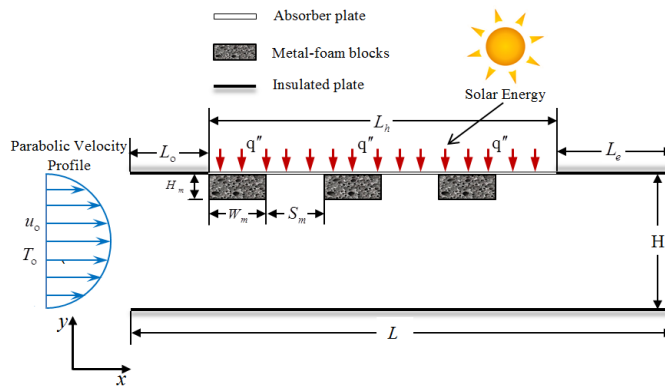


Figure 1. Configuration Under Current Study.

The momentum equations includes both Brinkman and Forchheimer terms to incorporate the viscous and inertial effects in the porous matrix, while Navier-Stokes is the governing equation in the fluid domain. For simplification, the angle brackets representing volume-averaged variables are dropped in equation pertaining to the porous domain, for example u in the porous region is equivalent to \bar{u} . Continuity in the fluid region:

$$\frac{\partial u}{\partial x} + \frac{\partial v}{\partial y} = 0 \quad (1)$$

Continuity in the porous region:

$$\frac{\partial u}{\partial x} + \frac{\partial v}{\partial y} = 0 \quad (2)$$

Momentum equation in the Fluid region:

$$\rho \left(u \frac{\partial u}{\partial x} + v \frac{\partial u}{\partial y} \right) = - \frac{\partial p}{\partial x} + \mu \left(\frac{\partial^2 u}{\partial x^2} + \frac{\partial^2 u}{\partial y^2} \right) \quad (3)$$

$$\rho \left(u \frac{\partial v}{\partial x} + v \frac{\partial v}{\partial y} \right) = - \frac{\partial p}{\partial y} + \mu \left(\frac{\partial^2 v}{\partial x^2} + \frac{\partial^2 v}{\partial y^2} \right) \quad (4)$$

Momentum equation in the Porous region:

$$\frac{\rho}{\varepsilon^2} \left(u \frac{\partial u}{\partial x} + v \frac{\partial u}{\partial y} \right) = - \frac{\partial p}{\partial x} + \frac{\mu}{\varepsilon} \left(\frac{\partial^2 u}{\partial x^2} + \frac{\partial^2 u}{\partial y^2} \right) - \frac{\mu}{K} u - \frac{\rho F \varepsilon}{\sqrt{K}} |\bar{u}| u \quad (5)$$

$$\frac{\rho}{\varepsilon^2} \left(u \frac{\partial v}{\partial x} + v \frac{\partial v}{\partial y} \right) = - \frac{\partial p}{\partial y} + \frac{\mu}{\varepsilon} \left(\frac{\partial^2 v}{\partial x^2} + \frac{\partial^2 v}{\partial y^2} \right) - \frac{\mu}{K} v - \frac{\rho F \varepsilon}{\sqrt{K}} |\bar{u}| v \quad (6)$$

where $|\bar{u}| = \sqrt{u^2 + v^2}$

The properties of porous matrix of metal foam, K and F , for momentum equation are taken from Calmudi, (1998). These empirical correlations are shown as follows:

$$F = 0.00212 (1 - \varepsilon)^{-0.132} \left(\frac{d_f}{d_p} \right)^{-1.63} \quad (7)$$

$$\frac{K}{d_p^2} = 0.00073(1-\varepsilon)^{-0.224} \left(\frac{d_f}{d_p} \right)^{-1.11} \quad (8)$$

where d_f / d_p is also given as a function of the porosity:

$$\frac{d_f}{d_p} = 1.18 \sqrt{\frac{(1-\varepsilon)}{3\pi}} \frac{1}{G} \quad (9)$$

where G is the shape function:

$$G = 1 - e^{-(1-\varepsilon)/0.04} \quad (10)$$

It should be noted that different values of ε were chosen in this study which correspond to d_f and d_p values as shown in Table 1. F and K values which were calculated from equations (7) and (8) respectively which also are presented in Table 1. Corresponding fluid flow boundary conditions:

$$\text{inlet at } x=0: \quad u = u_o 6(y/H)^{1/2} - (y/H)^{1/4} \quad v = 0 \quad (\text{fully developed flow}) \quad (11a)$$

$$\text{lower plate at } y=0: \quad u = 0 \quad v = 0 \quad (\text{no-slip condition}) \quad (11b)$$

$$\text{upper plate at } y=H: \quad u = 0 \quad v = 0 \quad (\text{no-slip condition}) \quad (11c)$$

$$\text{exit at } x=L: \quad \frac{\partial u}{\partial x} = 0, \quad v = 0 \quad (\text{fully developed flow}) \quad (11d)$$

Matching conditions are applied at the fluid-porous interface, (i.e. the continuity of velocity components and stresses are invoked). The governing energy equations are written for the metal-foam and fluid phase based on the local thermal equilibrium between them:

Energy equation in the fluid region:

$$u \frac{\partial T}{\partial x} + v \frac{\partial T}{\partial y} = \frac{k}{\rho c_p} \left(\frac{\partial^2 T}{\partial x^2} + \frac{\partial^2 T}{\partial y^2} \right) \quad (12)$$

Energy equation porous region:

$$u \frac{\partial T}{\partial x} + v \frac{\partial T}{\partial y} = \frac{k_{eff}}{\rho c_p} \left(\frac{\partial^2 T}{\partial x^2} + \frac{\partial^2 T}{\partial y^2} \right) \quad (13)$$

where $k_{eff} = \varepsilon k_f + (1-\varepsilon)k_s$. Corresponding energy boundary conditions:

$$\text{inlet} \quad (x=0): \quad T = T_o \quad (14a)$$

$$\text{lower plate } (y=0): \quad \left. \frac{\partial T}{\partial y} \right|_{y=0} = 0 \quad (14b)$$

$$\text{upper plate } (y=H): \quad \left. \frac{\partial T}{\partial y} \right|_{y=H} = \begin{cases} 0 & \text{insulated walls} \\ -\frac{q''}{k_{eff}} & \text{horizontal walls adjacent to blocks} \\ -\frac{q''}{k} & \text{horizontal walls adjacent to fluid} \end{cases} \quad (14c)$$

$$\text{exit } (x=L): \quad \left. \frac{\partial T}{\partial x} \right|_{x=L} = 0 \quad (14d)$$

Continuity of temperatures and heat flux are also invoked at fluid-porous interface regions.

Nondimensional Form

The governing equations and closure conditions are normalized, utilizing the following parameters:

$$\begin{aligned} X &= \frac{x}{H}, \quad Y = \frac{y}{H} \\ U &= \frac{u}{u_*}, \quad V = \frac{v}{u_*}, \quad P = \frac{P}{\rho u_*^2}, \quad \theta = \frac{T - T_*}{q(H/k_{eff})} \\ R_c &= \frac{k_{eff}}{k}, \quad Da = \frac{K}{H^2}, \quad C = F \cdot \varepsilon, \quad Re = \frac{\rho u_* H}{\mu}, \quad Pr = \frac{\mu c_p}{k} \end{aligned}$$

Again, for simplification, the angle brackets representing volume-averaged variables are dropped in equation pertaining to the porous domain. Therefore, the normalized governing equations are as follows, continuity:

$$\frac{\partial U}{\partial X} + \frac{\partial V}{\partial Y} = 0 \quad (15)$$

Equations (2-5) may be combined in a single form for both fluid and porous domains and then written in a dimensionless form as:

Momentum:

$$\frac{1}{\varepsilon^2} \left(U \frac{\partial U}{\partial X} + V \frac{\partial U}{\partial Y} \right) = -\frac{\partial P}{\partial X} + \frac{1}{\varepsilon \cdot Re} \left(\frac{\partial^2 U}{\partial X^2} + \frac{\partial^2 U}{\partial Y^2} \right) - \frac{1}{Da \cdot Re} U - \frac{C}{\sqrt{Da}} |\vec{U}| U \quad (16)$$

$$\frac{1}{\varepsilon^2} \left(U \frac{\partial V}{\partial X} + V \frac{\partial V}{\partial Y} \right) = -\frac{\partial P}{\partial Y} + \frac{1}{\varepsilon \cdot Re} \left(\frac{\partial^2 V}{\partial X^2} + \frac{\partial^2 V}{\partial Y^2} \right) - \frac{1}{Da \cdot Re} V - \frac{C}{\sqrt{Da}} |\vec{U}| V \quad (17)$$

In fluid region, the porosity ε and the Darcy number Da are respectively set equal to unity and infinity. Boundary conditions are:

$$\text{inlet at } X = 0 : \quad U = 6(Y)[1 - Y] \quad V = 0 \quad (18a)$$

$$\text{lower plate at } Y = 0 : \quad U = 0 \quad V = 0 \quad (18b)$$

$$\text{upper plate at } Y = 1/2 : \quad U = 0 \quad V = 0 \quad (18c)$$

$$\text{exit at } X = L/D_h : \quad \frac{\partial U}{\partial X} = 0 \quad V = 0 \quad (18d)$$

Similar to the flow field, the governing Eqs. (11) and (12) for the thermal field are combined into a single equation as follows:

$$U \frac{\partial \theta}{\partial X} + V \frac{\partial \theta}{\partial Y} = \frac{R_c}{\text{Re Pr}} \left(\frac{\partial^2 \theta}{\partial X^2} + \frac{\partial^2 \theta}{\partial Y^2} \right) \quad (19)$$

where R_c is set to unity in the fluid region. Non-dimensional boundary conditions are:

$$\text{inlet at } X = 0 : \quad \theta = 0 \quad (20a)$$

$$\text{lower plate at } Y = 0 : \quad \left. \frac{\partial \theta}{\partial Y} \right|_{Y=0} = 0 \quad (20b)$$

$$\text{upper plate at } Y = 1/2 : \quad \left. \frac{\partial \theta}{\partial Y} \right|_{y=1/2} = \begin{cases} 0 & \text{insulation walls} \\ -\frac{1}{R_c} & \text{horizontal walls adesent to blocks} \\ -1 & \text{horizontal walls adesent to fluid} \end{cases} \quad (20c)$$

$$\text{exit at } X = L/D_h : \quad \left. \frac{\partial \theta}{\partial X} \right|_{X=L/D_h} = 0 \quad (20d)$$

NUMERICAL METHOD

The governing equations and the boundary conditions are numerically solved using the commercial software COMSOL Multiphysics 5.2a which utilizes finite element method (FEM). The temperature, fluid velocity and the heat flux at the solid-fluid interface were coupled using multiphysics module. Triangular elements with minimum size of 4×10^{-4} are considered for meshing. Furthermore, highly packed mesh near the metal foam blocks and walls are utilized to capture the interface condition, wall temperature and heat flux.

RESULTS AND DISCUSSION

Results from our computational model were first compared with the numerical data from Chikh et al. (1998) for validation purposes. They studied an electronic cooling system using three regular, not metallic, porous blocks mounted on the lower plate of channel which is also heated through the lower plate (Figure 2). Comparison of streamlines with their work for $Re = 500$, $A = 4$, $R_y=0.25$, $R_x=0.5$, $H = 0.5$, $\varepsilon = 0.6$, $Pr = 0.7$ and two Darcy numbers are presented in Figure 2. As the permeability of the porous medium increases (i.e. $Da = 10^{-3}$) more fluid penetrates into the blocks. Additionally, the flow rate that goes into the first block is bigger compared to the flow rate passing through the other ones leading to enhancement of heat transfer as shown in figure 2(a). However, for low Darcy number ($Da \leq 10^{-5}$), the higher pressure of the flow in the area closer to the center of the channel compared to the area between the blocks results in recirculation of the fluid in these zones as shown in figure 2 (b). The resulting vortices prevents the fluid from flowing through the next porous block and as a result from the second block onwards, the metal foams tend to act relatively as solid non-permeable slabs.

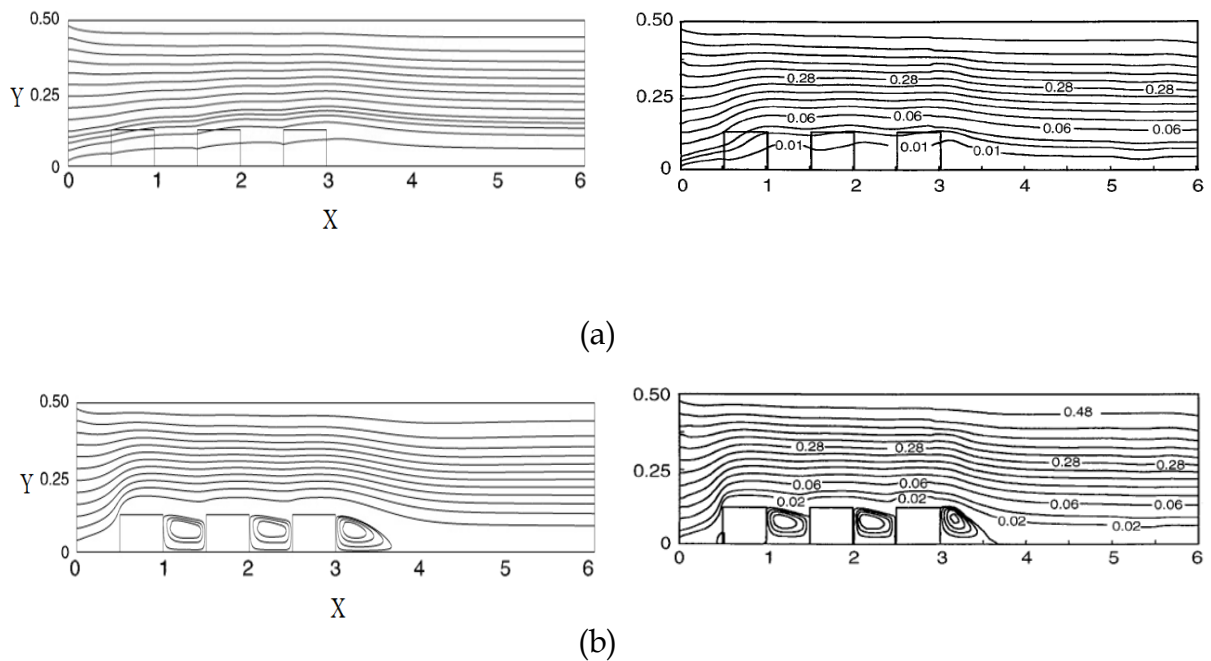


Figure 2. Streamlines Validation with Chikh et al. (1998) Results for The Same Stream Function Values at $Re = 500$, $R_x = 0.5$ and $A= 4$: (a) $Da = 10^{-3}$, (b) $Da=10^{-5}$.

Figure 3 (a) shows the comparison of the dimensionless wall temperature profile for $Re = 500$ and $A = 4$ with Chikh et al. (1998) for thermal conductivity ratios as high as $R_c = 100$. It is clearly shown that the presence of the porous blocks will reduce the wall temperature as the Da increases compared to the pure fluid case. For example, when $Da = 10^{-3}$ and $Da = 10^{-5}$ the average decrement in the wall

temperature was found to be 56% and 18% respectively compared to the case without any blocks.

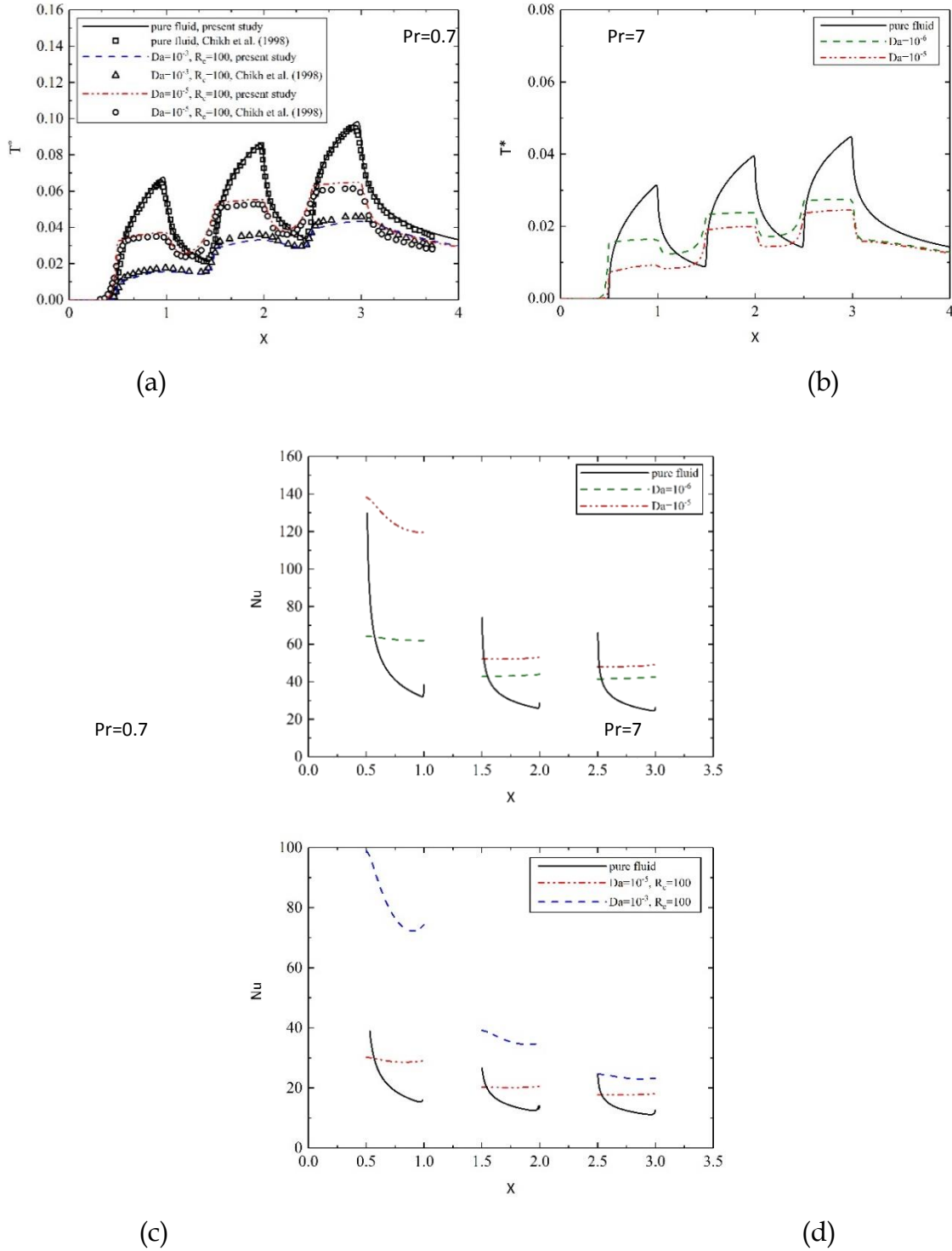


Figure 3. (a) Comparison of Dimensionless Wall Temperature with Those of Chikh et al. (1998) Results, (b) Dimensionless Wall Temperature Profile for Water Flow, (c and d) Local Nusselt Number Along The Axial Direction for $Re=500$ and $A=4$.

We increased Prandlt number from 0.7 (air) to 7 (water) (Figure 3 (b)); which leads to increase in the thermal entrance length and substantially decreases the wall temperature; which ultimately increases the Nusselt number, particularly in the first block as shown in figures 3 (c and d). When air is used, the average rate of heat transfer enhancement through the first block (compared to the case without porous blocks) is found to be 278% and 135%, for $Da = 10^{-3}$ and $Da = 10^{-5}$ respectively. Since using multiple blocks results in a considerable pressure drop penalty, it restricts their implementation for practical purposes. In other words, applying one porous block seems to be desirable for further energy efficiency in certain thermal applications with limitations on the pumping power, such as electronic cooling. Nevertheless our results are in very good agreement with Chikh et al. (1998) numerical results, which establishes our computational model as robust and reliable to study the setting at hand.

The aluminum foam heat sinks are employed in the present study as shown in figure 1. The solid materials are made of aluminum-alloy and its corresponding properties are shown in table 1. Water is used as the working fluid ($\rho=998.2 \text{ kg/m}^3$ and $k=0.6 \text{ W/m K}$). The effect of some important parameters such as porosity ($0.85 \leq \varepsilon \leq 0.95$), Darcy number ($1.72 \times 10^{-5} \leq Da \leq 4.58 \times 10^{-5}$) and Reynolds number ($250 \leq Re \leq 1000$) on the hydrodynamic and thermal behavior of the model is explored. Furthermore, the fluid enters the channel with uniform temperature and parabolic velocity profile representing fully developed conditions. To illustrate the effect of the aforementioned physical parameters, results (Nu and the flow) are only presented in the area with the blocks and the heat source as well as their vicinity.

Table 1. Properties of Metal-Foams for Various Porosities. Calmidi et al. (2000)

metal-foam	ε	d_f (mm)	d_p (mm)	Da	F	ρ (kg/m^3)	k (W/m K)
aluminum-alloy T6201	0.85	0.4	2.62	1.72E-05	0.058		
	0.90	0.4	3.02	2.92E-05	0.078	2690	
	0.95	0.4	3.32	4.58E-05	0.099		218

Figure 4 shows the local Nusselt number along the heated wall for aluminum-alloy T6201. As Darcy number increases the heat exchange rate between the solid and the fluid phases inside the porous metal-foam region becomes more considerable. It can be seen from figure 4 that the Darcy number has a significant impact on the local Nusselt number distribution, especially inside the first metal-foam block. As porosity increases to 0.95 and subsequently Da increases to 4.58×10^{-5} , the average rate of increment in the Nusselt number was found to be 13%. Therefore, it can be concluded that Darcy number plays a prominent role in heat transfer enhancement of the porous metal foam compared to lower porosity cases.

Figure 4 (b) shows the local Nusselt number for $\varepsilon=0.95$ and $Da=4.58 \times 10^{-5}$ at different Reynolds numbers. It is clear that the Nusselt number is directly

proportional to the Re. The maximum enhancement ($Nu_{Re=1000}/Nu_{Re=250}$) in this study was found to be 301% at $\epsilon = 0.95$.

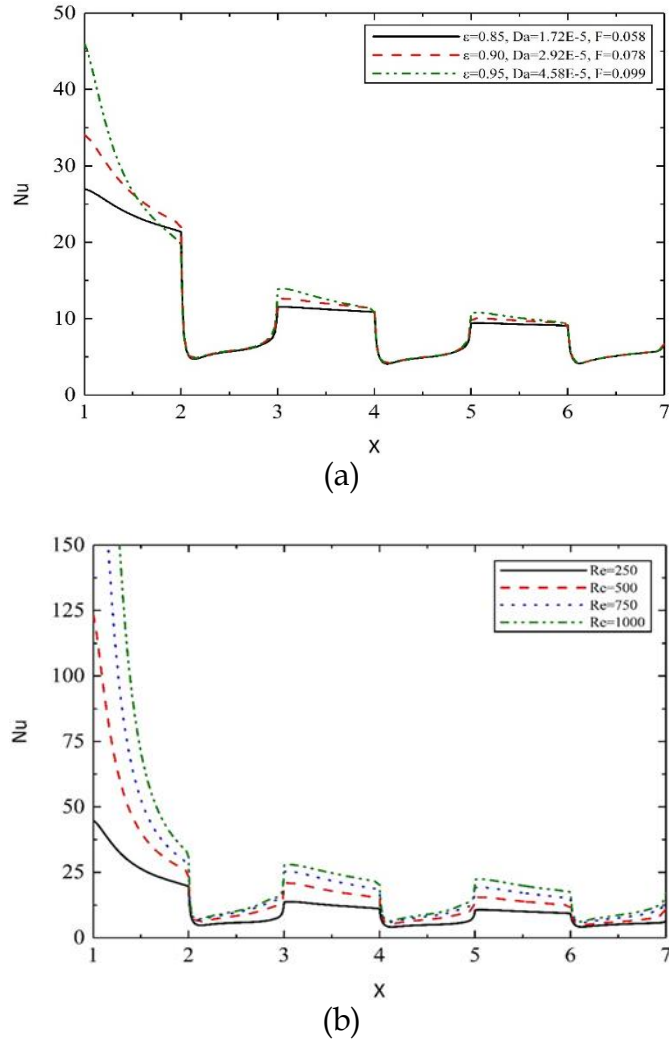


Figure 4. Local Nusselt Number Along The Channel Axis for Aluminum-Alloy T6201 at: (a) $Re=250$ and Different Porosities, (b) $\epsilon = 0.95$, $Da=4.58\times 10^{-5}$, $F=0.099$ and Different Reynolds Number.

Figure 5 shows the streamlines and dimensionless temperature contours for different Reynolds numbers. At high Reynolds numbers (i.e. $Re=1000$), the size of recirculation zones between the blocks increases and their center is pushed towards channel central region. From the isotherm contours, highest values of isothermal lines are localized near the heated wall and gradually fading towards the core region, due to the fact that the conduction heat transfer is more dominant in this part. As such, the temperature gradient and isothermal density near the wall increases when Reynolds number increases.

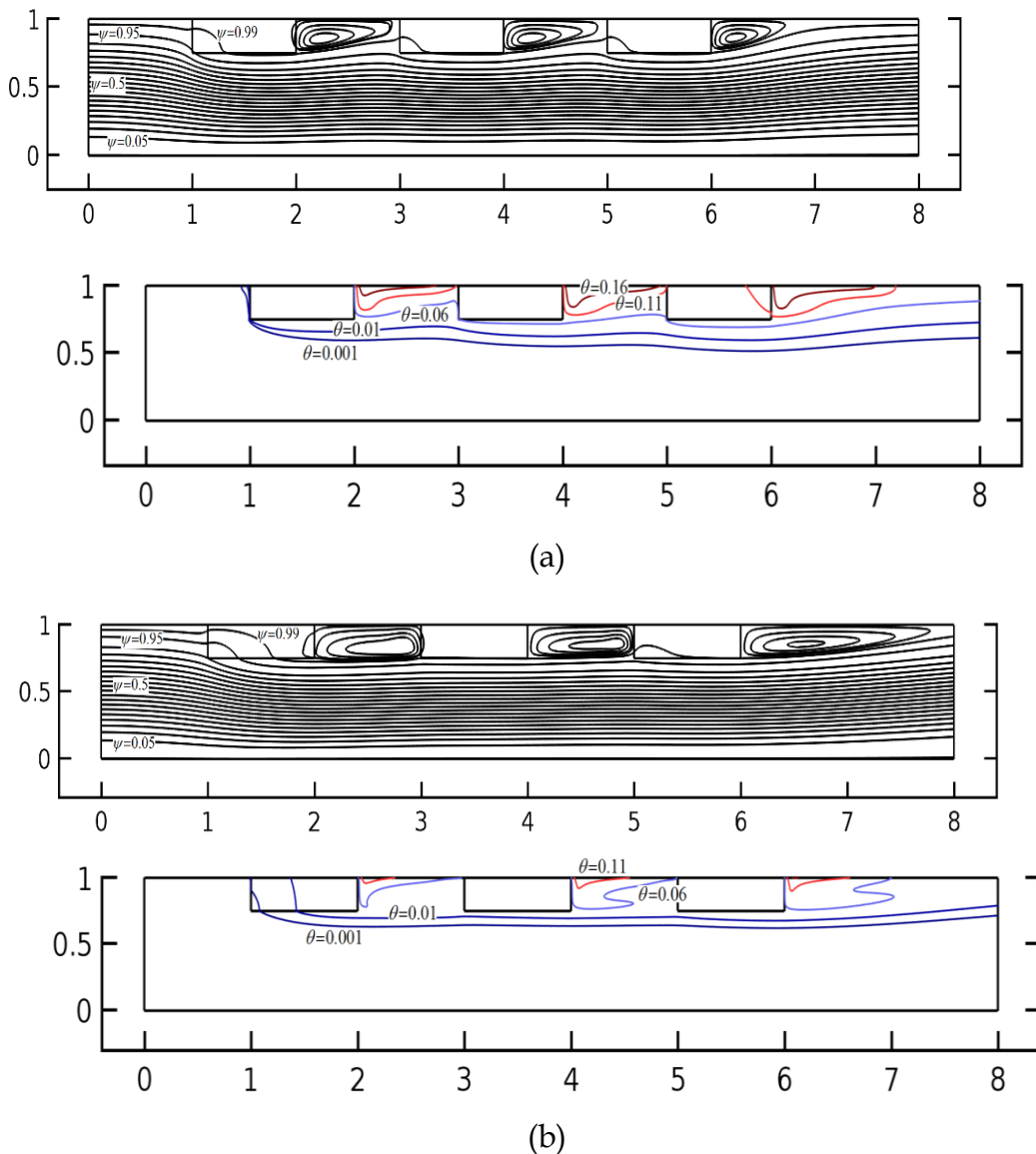


Figure 5. Streamlines and Dimensionless Temperature Contours Respectively for $\epsilon = 0.95$, $Da = 4.58 \times 10^{-5}$ and $F = 0.099$ at: (a) $Re = 250$, (b) $Re = 1000$.

CONCLUSION

Heat transfer in a parallel-plate solar water channel with integrated aluminum-alloy metal foam blocks has been studied numerically. For the porous region, the Brinkman-Forchheimer extension of the Darcy law was applied while Local thermal equilibrium was assumed between water, as the working fluid and the metallic porous section. Our results show that Darcy number plays a significant role in heat transfer enhancement compared to parameters such as porosity or the inertial coefficient of the blocks. Moreover, it is observed that most of the enhancement is resulted from the interactions between the fluid and the first porous block. Therefore, one block would be a better choice in certain applications

with pumping power limitations. The maximum thermal enhancement for the studied configurations shows 3 times increase in Nusselt number compared to the case with no blocks. Based on the results, metal foam heat exchangers can be considered as a promising solution to increase heat transfer enhancement in applications such as solar collectors and electronic cooling applications.

RECOMMENDATIONS

Nanofluids flow such as Al₂O₃ can be considered as an extra type of heat transfer enhancement coupled with metal-foam blocks.

REFERENCES

- Albojamal, A., Vafai, K. (2017) 'Analysis of single phase, discrete and mixture models, in predicting nanofluid transport', International Journal of Heat and Mass Transfer, Vol. 114, pp. 225-237. <http://www.sciencedirect.com/science/article/pii/S001793101732077X>
- Angirasa, D.(2002) 'Forced Convective Heat Transfer in Metallic Fibrous Materials', Journal of Heat Transfer, Vol. 124, pp. 739-745. <http://heattransfer.asmedigitalcollection.asme.org/article.aspx?articleid=1445893>
- Banhart, J. (2001) 'Manufacture, characterisation and application of cellular metals and metal foams', Progress in Materials Science, Vol. 46, pp. 559-632. <http://www.sciencedirect.com/science/article/pii/S0079642500000025>
- Bashria, A., Yousef, A., Adam, N.M., Sopian, K., Zaharim , A., Alghoul, M. (2007) 'Analysis of Single and Double Passes V-Grooves Solar Collector With and Without Porous Media', International Journal of energy and environment, Vol. 1, pp. 109-114. <https://www.researchgate.net/publication/241906626>
- Calmidi, V. V. (1998). Transport phenomena in high porosity metal foams. Ph.D. Thesis, University of Colorado, Boulder, CO. Retrieved from <http://abcm.org.br/anais/encit/2000/arquivos/palestras/mahajan.pdf>
- Calmidi, V. V., & Mahajan, R. L. (2000). Forced convection in high porosity metal foams. Retrieved from <http://heattransfer.asmedigitalcollection.asme.org/article.aspx?articleid=1444400>
- Chabane, F., Hatraf, N., Moumami, N. (2014) 'Experimental study of heat transfer coefficient with rectangular baffle fin of solar air heater', Front. Energy, Vol. 8, pp. 160-172. <https://link.springer.com/article/10.1007/s11708-014-0321-y>
- Chikh, S., Boumedien, A., Bouhadef, K., Lauriat , G. (1998) 'Analysis of fluid flow and heat transfer in a channel with intermittent heated porous blocks', Heat and Mass Transfer, Vol. 33, pp. 405-413. <https://link.springer.com/article/10.1007/s002310050208>
- Kalogirou, S.A. (2004) 'Solar thermal collectors and applications', Progress in Energy and Combustion Science, Vol. 30, pp. 231-295. <http://www.sciencedirect.com/science/article/pii/S0360128504000103>

- Kudish, A.I., Evseev, E.G., Walter, G., Leukefeld, T. (2014) 'Simulation study of a solar collector with a selectively coated polymeric double walled absorber plate', *Energy Conversion and Management*, Vol. 43, pp. 651-671.
<http://www.sciencedirect.com/science/article/pii/S0196890401000668>
- Lee, D.Y., Vafai, K. (1999) 'Analytical characterization and conceptual assessment of solid and fluid temperature differentials in porous media', *International Journal of Heat and Mass Transfer*, Vol. 42, pp. 312-324.
<http://www.sciencedirect.com/science/article/pii/S0017931098001859>
- Lu, T.J., Stone, A.H., Ashby, M.F. (1998) 'Heat transfer in open-cell metal foams', *Acta mater*, Vol. 46, pp. 3619-3635.
<http://www.sciencedirect.com/science/article/pii/S1359645498000317>
- Lu, W., Zhang, T., Yang, M., Wu, Y. (2017) 'Analytical solutions of forced convective heat transfer in plate heat exchangers partially filled with metal foams', *International Journal of Heat and Mass Transfer*, Vol. 110, pp. 476-481.
<http://www.sciencedirect.com/science/article/pii/S0017931016326060>
- Lu, W., Zhao, C.Y., Tassou, S.A. (2006) 'Thermal analysis on metal-foam filled heat exchangers. Part I: Metal-foam filled pipes', *International Journal of Heat and Mass Transfer*, Vol. 49, pp. 2751-2761.
<http://www.sciencedirect.com/science/article/pii/S0017931006000524>
- Patankar, S.V. (1980) 'Numerical heat transfer and fluid flow', Mc Graw Hill, New York.
- Qu, Z.G., Xu, H.J., Tao, W.Q. (2012) 'Fully developed forced convective heat transfer in an annulus partially filled with metallic foams: An analytical solution', *International Journal of Heat and Mass Transfer*, Vol. 55, pp. 7508-7519.
<http://www.sciencedirect.com/science/article/pii/S0017931012005844>
- Reddy, K.S., Satyanarayana, G.V. (2008) 'Numerical study of porous finned receiver for solar parabolic through concentrator', *Engineering Applications of Computational Fluid Mechanics*, Vol. 2, pp. 172-184.
<https://www.researchgate.net/publication/308086401>
- Wang, V.C., Chen, C.K. (2002) 'Forced convection in a wavy-wall channel', *International Journal of Heat and Mass Transfer*, Vol. 45, pp. 2587-2595.
<http://www.sciencedirect.com/science/article/pii/S0017931001003350>
- Xu, H., Gong, L., Huang, S., Xu, M. (2015) 'Flow and heat transfer characteristics of nanofluid flowing through metal foams', *International Journal of Heat and Mass Transfer*, Vol. 83, pp. 399-407.
<http://www.sciencedirect.com/science/article/pii/S0017931014011144>
- Zhao, C.Y. (2014) 'Review on thermal transport in high porosity cellular metal foams with open cells' *International Journal of Heat and Mass Transfer*, Vol. 55, pp. 3618-3632.
<http://www.sciencedirect.com/science/article/pii/S0017931012001664>